Since January 2020 Elsevier has created a COVID-19 resource centre with free information in English and Mandarin on the novel coronavirus COVID-19. The COVID-19 resource centre is hosted on Elsevier Connect, the company's public news and information website.

COVID-19 in people with neurofibromatosis 1, neurofibromatosis 2, or schwannomatosis

Jineta Banerjee, Jan M. Friedman, Laura J. Klesse, Kaleb Yohay, Justin T. Jordan, Scott Plotkin, Robert J. Allaway, Jaishri O. Blakeley

PII: S1098-3600(22)00988-1

DOI: https://doi.org/10.1016/j.gim.2022.10.007

Reference: GIM 324

To appear in: *Genetics in Medicine*

Received Date: 10 May 2022

Revised Date: 11 October 2022

Accepted Date: 12 October 2022

Please cite this article as: Banerjee J, Friedman JM, Klesse LJ, Yohay K, Jordan JT, Plotkin S, Allaway RJ, Blakeley JO, COVID-19 in people with neurofibromatosis 1, neurofibromatosis 2, or schwannomatosis, *Genetics in Medicine* (2022), doi: https://doi.org/10.1016/j.gim.2022.10.007.

COVID-19 in people with neurofibromatosis 1, neurofibromatosis 2, or schwannomatosis

Jineta Banerjee[1], Jan M. Friedman[2], Laura J. Klesse[3], Kaleb Yohay[4], Justin T Jordan[5], Scott Plotkin[6], Robert J Allaway[1,*], Jaishri O Blakeley[7,*]

[1]*Sage Bionetworks, Seattle, WA*

[2]*Department of Medical Genetics, Faculty of Medicine, University of British Columbia, Vancouver, BC*

[3]*Department of Pediatrics and Neurosurgery, Simmons Cancer Center, University of Texas Southwestern Medical Center, Dallas, TX*

[4]*Comprehensive Neurofibromatosis Center at NYU Langone Health, New York, NY*

[5]*Department of Neurology, Massachusetts General Hospital, Boston, MA*

[6]*Stephen E. and Catherine Pappas Center for Neuro-Oncology, Massachusetts General Hospital, Boston, MA*

[7]*Departments of Neurology, Oncology, and Neurosurgery, Johns Hopkins University School of Medicine, Baltimore, MD*

** co-corresponding authors*

Co-Corresponding authors:

Jaishri O Blakeley

Email: jblakel3@jhmi.edu

Phone: 410-955-6827

Address: The Johns Hopkins University School of Medicine, 600 N. Wolfe Street, Meyer Building, Room 8-149, Baltimore, Maryland - 21287

Robert J Allaway

Email: robert.allaway@sagebionetworks.org,

Phone: 206-928-8231

Address: 2901 Third Ave, Suite 330, Seattle, Washington - 98121

ABSTRACT

Purpose: People with pre-existing conditions may be more susceptible to severe Coronavirus disease 2019 (COVID-19) when infected by severe acute respiratory syndrome coronavirus- 2 (SARS-CoV-2). The relative risk and severity of SARS-CoV-2 infection in people with rare diseases like neurofibromatosis (NF) type 1 (NF1), neurofibromatosis type 2 (NF2), or schwannomatosis (SWN) is unknown.

Methods: We investigated the proportions of SARS-CoV-2 positive or COVID-19 patients in people with NF1, NF2, or SWN in the National COVID Collaborative Cohort (N3C) electronic health record dataset.

Results: The cohort sizes in N3C were 2,501 (NF1), 665 (NF2), and 762 (SWN). We compared these to N3C cohorts of other rare disease patients (98 - 9844 individuals) and the general non-NF population of 5.6 million. The site- and age-adjusted proportion of people with NF1, NF2, or SWN who tested positive for SARS-CoV-2 or were COVID-19 patients (collectively termed *positive cases*) was not significantly higher than in individuals without NF or other selected rare diseases. There were no severe outcomes reported in the NF2 or SWN cohorts. The proportion of patients experiencing severe outcomes was no greater for people with NF1 than in cohorts with other rare diseases or the general population.

Conclusion: Having NF1, NF2, or SWN does not appear to increase the risk of being SARS-CoV-2 positive or of being a COVID-19 patient, or of developing severe complications from SARS-CoV-2.

Keywords: COVID-19, SARS-CoV-2, rare disease, Neurofibromatosis type-1, NF1, Neurofibromatosis type-2, NF2, Schwannomatosis, electronic health records (EHR)

INTRODUCTION:

Neurofibromatosis type 1 (NF1), neurofibromatosis type 2 (NF2) and schwannomatosis (SWN) are autosomal dominant genetic conditions predisposing patients to tumors involving the central and peripheral nervous system. NF1 is much more common (estimated prevalence of 1/3600) than NF2 (1/56,000) or SWN (1/126,000).[1,2] Given that NF1, NF2, and SWN often cause chronic health impairments, the care community has been concerned about the possibility of increased risk of infection or severe outcomes of COVID-19 in people with one of these genetic conditions. While these diseases do not generally cause immunosuppression and therefore may not increase susceptibility to SARS-CoV-2 infection, other factors could increase risks associated with COVID-19 in people with NF. For instance, NF1 is associated with several types of malignant tumors (e.g., malignant peripheral nerve sheath tumors, juvenile myelomonocytic leukemia and glioma), non-malignant tumors, and a range of other manifestations (e.g., vasculopathy and cognitive deficits). People with NF1 have a reduced life expectancy attributed predominantly to premature death caused by cancer or vasculopathy.[3,4] Some of these manifestations might increase risks associated with SARS-CoV-2 infection. People with NF1 have also been impacted by access to routine care and delayed activity in clinical trials during the COVID-19 pandemic,[5,6] but it is still unknown if people with NF1, NF2, or SWN are more susceptible to severe acute respiratory syndrome-coronavirus-2 (SARS-CoV-2) infection or more likely to have severe symptoms of the disease than other populations.

To address these questions, we explored the electronic health records (EHR) of people with NF1, NF2, or SWN in the National COVID Cohort Collaborative (N3C) Data Enclave[7] to estimate the proportion of patients with these diagnoses affected by SARS-CoV-2 or COVID-19. The N3C Enclave is a dataset and analysis platform that permits researchers to access, query, and analyze COVID-19-related EHR data (including standardized clinical diagnoses, laboratory results, medication records, procedures, and visit records) from 55 participating healthcare sites and an estimated 6.4 million individuals in the United States (to July 2021)[7,8] to better understand the impact of COVID-19 on specific populations.

This study explores the proportions of SARS-CoV-2 positive or COVID-19 positive patients in people with NF1, NF2, and SWN. Further, we examine the proportions of positive cases with NF1 who experienced high severity of COVID-19 disease based on the retrospective observational data available in N3C.

MATERIALS AND METHODS:

Data access

Data access and analysis were compliant with Sage Bionetworks protocol granted IRB-exempt status by the Western Institutional Review Board - Copernicus Group (WCG) IR, and data access request approved by the N3C Enclave Data Access Committee. All cohorts were generated using custom SQL queries and subsequently analyzed in the N3C Data Enclave. Some of the aggregate data were downloaded after approval by the

N3C data access committee and further analyzed in a private, secure cloud computing instance provisioned by Sage Bionetworks. The data analyzed in this study were last updated on July 29, 2021.

SARS-CoV-2 positive or COVID-19 patient criteria

Patients were documented as SARS-CoV-2 positive or COVID-19 patients (together called *positive cases*) in the N3C Data Enclave if they had a hospital visit after 1/1/2020 and had one or more of the following: 1) a positive result from one or more of a set of predefined SARS-CoV-2 laboratory tests, 2) a “strong positive” COVID-19 diagnostic code from the ICD-10 or SNOMED tables described in Version 3.3 of the N3C Phenotype Documentation[9], or 3) two “weak positive” COVID-19 diagnostic codes from the ICD-10 or SNOMED tables in the phenotype documentation during the same encounter or on the same date prior to 5/1/2020. In cases where a patient had both a positive laboratory test result and a positive COVID-19 diagnosis code, priority was given to the criteria that had an earlier date. In cases where a patient had both positive test results and COVID-19 diagnosis code documented on the same date, priority was given to the positive laboratory test result. Since one criterion was selected and documented for each patient to determine their SARS-CoV-2 or COVID-19 status, there was no duplication of individuals if they satisfied more than one criterion.

Each positive case entered in N3C was matched to two SARS-CoV-2-negative patients *(controls)* at the same site by age, gender, and race. *Control* patients met one or more of the following criteria: 1) set of predefined SARS-CoV-2 laboratory tests with a non-

positive result, 2) did not qualify as a COVID-19 patient, or 3) had at least 10 days between the minimum and maximum encounter date to eliminate patients who were only seen for a COVID test. The N3C cohort and case definition criteria are publicly available as described in version 3.3 of the N3C COVID-19 Phenotype Documentation (https://github.com/National-COVID-Cohort-Collaborative/Phenotype_Data_Acquisition/wiki/Latest-Phenotype).

Case-control matching at the clinical contributing site:

Matching of positive cases and controls was done on-site at the clinical centers before any data was deposited into the N3C data enclave. The phenotype and data acquisition workstream of N3C defined the phenotype and provided the participating sites with programmatic scripts for the matching of SARS-CoV2 positive and negative patients. All of the code used to select the cohort and match are available on GitHub (https://github.com/National-COVID-Cohort-Collaborative/Phenotype_Data_Acquisition/tree/master/PhenotypeScripts). Briefly, the code scripts were applied first to select the positive case, then potential match controls at the site depositing records for the positive case. Patients who were qualified to be controls had at least one negative COVID test, never had a positive COVID test, or did not have U07.1 (COVID) diagnosis code in their record. The scripts iterated through three rounds of matching, using progressively looser demographic criteria until either every case had two matched controls, or the dataset ran out of possible controls. For example, the script attempted to match cases to controls on race, age group, ethnicity, and sex. If two matches could not be found using those criteria, then only matching

race, age group, and sex was attempted. If two matches are still not possible, then matching was done on age and sex. If two matches were still not found, then the cases and controls were only matched on sex. At this point, essentially everyone in the case group had two matched controls, but it is possible that there may be cases that did not if the site ran out of controls (publication[7] and personal communication).

Patient cohort selection

Patients included in the N3C dataset consist of positive cases and controls from same contributing sites in the ratio 1:2, matched by age, gender (Female, Male, Unknown), race (White, Black or African-American, Native Hawaiian or Pacific Islander, Asian, Other, Missing/Unknown) and ethnicity (Hispanic, Non-Hispanic, Missing/Unknown) (N3C COVID-19 Phenotype version 3.3).[7,8]

In this study, the dataset was stratified by disease, selecting several disease cohorts as comparison groups. An NF1-specific concept set was constructed using neurofibromatosis type 1-relevant diagnosis codes (Supplemental Table 1) from SNOMED, ICD9/10, LOINC, and Nebraska Lexicon (N3C Codeset ID: 792972142). Any unique person in the N3C dataset (identified by their unique N3C person ID) with diagnosis codes belonging to any of the NF1-relevant concepts in the concept set defined by the study team (24 concepts; Supplemental Table 1) was included in the NF1 cohort. This was repeated for neurofibromatosis type 2 (NF2) and schwannomatosis (SWN) as well as the other comparison cohorts.

Our comparison cohorts included patients with other rare diseases like fragile X syndrome (FXS), tuberous sclerosis (TSC), Merkel cell carcinoma (MCC), or acute myeloid leukemia (AML); as well as non-rare diseases like diabetes mellitus type 1 (DM1) or controlled hypertension (HYP), the N3C population without NF1 (Non-NF1), without NF2 (Non-NF2), or without SWN (Non-SWN). We selected TSC, FXS, MCC, and AML as comparison groups that are rare diseases and could potentially account for any biases associated with disease groups of small numbers with chronic conditions. TSC, like NF1, is an inherited autosomal dominant disease, and is closely related to NF1 among neurocutaneous syndromes in both genetic aspects and the presentation of symptoms and diagnosis in childhood[10]. Likewise, FXS is a rare X-linked dominant disease that is diagnosed in childhood.[11] MCC and AML represent rare cancers[12,13] which have molecular similarities to malignancies associated with NF1, NF2, and SWN. We also wanted to compare the rare disease cohorts to other larger disease groups with known association with COVID-19 severity (as positive controls). This led us to selecting DM1 and HYP groups which were well established co-morbidities that showed higher risk of COVID-19 severity. The non-NF1, non-NF2, and non-SWN groups were included to represent the general N3C population.

The concept sets generated for NF1, NF2, and SWN primarily included individuals with confirmed diagnosis of the conditions but also included individuals that presented with conditions associated with these diseases, possibly indicating they had NF1, NF2, or SWN. This was to ensure that we did not miss an association of the disease and positive cases (and to optimize our cohort selection for sensitivity); a summary of the

clinical concepts and their association with the included patients in the NF1, NF2, and SWN cohorts is available in Supplemental Figure 1. All concept sets are available in Supplemental Tables 1-9.

Patients with missing data for pre-existing diagnosis, SARS-CoV-2 test, COVID-19 diagnosis, or age were excluded from the analysis. Due to data anonymization prior to contribution to the N3C database, if a patient visited more than one of the 55 healthcare sites contributing to N3C, they would be treated as multiple unique patients (one per site). This is a known limitation of the dataset, but it is unknown if this scenario occurred in the present analysis. Additionally, the selected cohorts are not mutually exclusive. A patient with DM1 and HYP were counted in both cohorts. This known limitation of our dataset was of low consequence since this study did not aim to look at interaction of diseases but only investigated proportions across any of the selected diseases.

Considerations and adjustments for the selected cohorts

The N3C dataset contains positive cases and controls in the ratio of 1:2 matched by age, gender, and race. Due to this inclusion criteria, the analyses in this study cannot accurately estimate the absolute incidence or prevalence of COVID-19 in selected disease cohorts. Additional factors introducing observation bias into the dataset include 1) the site contributing data, and 2) patients' age (which contributes to both COVID-19 susceptibility and disease severity as well as the development of symptoms related to NF1, NF2, or SWN, and a recorded diagnosis of these conditions).

1) Site related adjustment for selected disease cohorts

Contributing sites may introduce observation bias into the contributed dataset due to the nature of patient population or geographical region or scale of the site. They may also introduce confounding factors into disease severity metrics, e.g., there may be variability of criteria in indications for intubation at various health care sites or availability of a given resource or procedure across sites. Additionally, data coming from some sites may not include certain variables due to various reasons like data not being collected, data not being coded properly, or particular data columns not being submitted to N3C. These data are missing but the occurrence of such missing variables is not at random and outside of our control. To adjust for these differences and missingness, we included patient data only from sites that contributed NF1, NF2, or SWN patients. To achieve this, first, the unique "data partner ids" (correlating to healthcare sites) in the NF1, NF2, and SWN cohorts were noted. These data partner ids were then used to filter all the other cohorts so that only patients contributed by sites that contributed NF1, NF2, or SWN patients were included.

2) Age adjustment for selected disease cohorts

The age-related differences between cohorts were adjusted by stratifying the cohorts into 10-year age bins. Each stratum was then weighted using the age-adjusted rate ("aarate") formula based on US standard population (US Census 2000)[14–20]. Each age-adjusted cohort comprised of the ages x through y and was calculated using the following formula:

$$aarate_{x-y} = \sum_{i=x}^{y} \left[\left(\frac{count_i}{population_i} \right) \times 100{,}000 \times \left\lfloor \frac{std\ population_i}{\sum_{j=x}^{y} std\ population_j} \right\rfloor \right]$$

Age-adjusted counts of positive cases, severe outcomes, or invasive ventilation for each cohort, and further details of calculation of age-adjustment are available as supplemental tables 11,12, and 13.

Bootstrap analyses

Three main groups of comparisons were assessed: *NF1 vs all other study cohorts*, *DM1 vs all other study cohorts*, and *NF1 vs all other "rare" cohorts (TSC, FXS, MCC, AML, NF2, SWN).* For the *NF1 vs all* comparison, a test vector was populated with the age-adjusted proportions from all the separate age strata of the NF1 cohort. A comparison vector was populated with the age-adjusted proportions for all the age strata in all the other cohorts. A Shapiro-Wilk test (base R v3.6.3 `shapiro.test` function) was used to test the normality of the distributions of the age-adjusted proportions in the different age strata for each cohort (NF1 cohort: p-value = 0.165, Shapiro-Wilk test). The age-adjusted proportions in the test and comparison vectors were compared to estimate the p-value of the real observations ("real p-value") (using the BSDA v1.2.0 `z.test` function). Then, the age-adjusted proportions in the test and comparison vectors were resampled 10,000 times to produce 10,000 possible combinations of age-adjusted proportions (using the `gdata v2.18.0 resample` function). For each "resampled cohort", a z-test was performed to estimate the distribution of possible p-values generated from the observed proportions. This distribution of p-values generated through bootstrap presents the confidence intervals

for the observed "real" p-value (i.e. the null distribution of the p-value)[21–24]. If the “real” p-value was less than p=0.05 but not significantly different from the distribution of various p-values generated in the bootstrap (Wilcoxon rank sum test), the cohorts in the comparison were considered significantly different with the real p-value unlikely to occur by chance (See supplementary methods for more details on the method and the rationale).

A similar approach was taken for all other comparisons, except that a non-parametric Wilcoxon rank sum test (base R v3.6.3 `wilcox.test function)` was used to estimate the real p-value for comparisons of severe outcomes and invasive ventilation (due to non-normal distribution in all cohorts). All real p-values were adjusted to correct for the number of overlapping comparisons for each disease using Benjamini-Hochberg method (BH). The distributions of bootstrapped p-values were visualized using R `ggplot2 v3.3.2`. Similar analyses were also done for NF2 and SWN cohorts.

Confidence interval calculations

All comparisons were tested using 95% confidence interval (CI) as default. In some bootstrap analysis comparisons, the skewed distribution of values did not allow CI calculations at 95% (as the difference between $\boldsymbol{\alpha}$ achieved from the distribution and $\boldsymbol{\alpha}_{\text{target}}$ was greater than $\boldsymbol{\alpha}_{\text{target}}/2$, where $\boldsymbol{\alpha}_{\text{target}} = 0.05$). In such cases, the highest CI that was able to be calculated is reported (60%). It should be noted that a 60% confidence interval is more likely to reject the null hypothesis compared to a 95% CI. In this study

CI were calculated and are reported at 95%, any comparisons with 60% CI have been explicitly noted in the tables.

RESULTS:

Demographics of the NF1, NF2, and SWN cohorts are comparable to those of other cohorts in N3C

From 6.4 million patients present in N3C Data enclave (v3.3, July 2021), we selected cohorts of rare (NF1: 2,501, NF2: 665, SWN: 762, TSC: 861, AML: 9,844, FXS: 98, MCC: 648) and non-rare diseases (non-NF1: 5.6 million, non-NF2: 5.6 million, non-SWN: 5.6 million, DM1: 66,234, HYP: 1.6 million) using concept sets of EHR diagnosis codes (Table 1, Fig. 1A). The FXS cohort was the smallest among the selected cohorts. Other rare disease cohorts were comparable in size but considerably smaller than the non-rare disease cohorts, as expected. The occurrence of NF1, NF2, and SWN patients in the N3C data (NF1: 0.0004 of total N3C patients, NF2: 0.0001 of total N3C patients, SWN: 0.0001 of total N3C patients) was higher than the expected population prevalence of these diseases (NF1: 0.0002[1,25–27], NF2: 0.00002[1], SWN: 0.000008[2] approximately), indicating that the N3C dataset may not represent a random sample of the general population (Supplemental Methods).

The distribution of ages of the selected rare and non-rare disease cohorts were significantly different (median ages provided in Table 1, Kruskal-Wallis rank sum test, p value < 2.2×10^{-16}). This suggests a need for age-adjustment of cohorts before

comparison. The NF1, NF2, and SWN cohorts were not significantly different from the non-NF1, non-NF2, or non-SWN cohorts in racial makeup, with a majority of white but a substantial representation from the black or African-American race (Figure 1B, Supplemental Table 10, Kruskal-Wallis rank sum test, p value = 0.94). The NF1, NF2, SWN, and the general population cohorts did not have significantly different distributions of male and female patients (Figure 1C, Supplemental Table 10, Kruskal-Wallis rank sum test, p value = 0.4159).

Age-adjusted proportion of SARS-CoV-2 positive cases in NF1, NF2, or SWN is not greater than other selected diseases.

To test whether SARS-CoV-2 affected the NF1 population differently than other populations, we compared the age-adjusted proportions of positive cases (SARS-CoV-2 positive and/or COVID-19 patients) in the NF1, NF2, and SWN cohorts individually with that of the non-NF population, other rare diseases, and selected non-rare disease cohorts (Figure 2, Supplemental Table 11, Table 1-2). The proportion of positive cases in the NF1 cohort was significantly different from other cohorts (Figure 2A, Table 1-2, Table 3, z-test p-value = 0.0028, BH adjusted p-value = 0.008) with a p-value unlikely to occur by chance (see Methods, bootstrap Wilcoxon p-value = 0.5). This suggests that the proportion of positive cases in the NF1 N3C cohort was not higher than the non-NF1 N3C cohort. Similarly, the NF2 cohort had a significantly lower proportion of positive cases than the non-NF2 cohort (Figures 2D, Table 2, z-test p-value = 3.9×10^{-5}, BH adjusted p-value = 1.2×10^{-4}, falls within bootstrap distribution: Wilcoxon p-value = 0.5). The age-adjusted proportions of positive cases in the SWN cohort, however, did not

differ significantly from the other cohorts (z-test p-value = 0.05, BH adjusted p-value = 0.16, and falls within bootstrap distribution: Wilcoxon p-value = 1.0, Figure 2G, Table 2). In contrast to NF1 and NF2, the proportion of positive cases observed in a non-rare disease like DM1 was not significantly different from the rest of the cohorts (z-test p-value = 0.15, BH adjusted p-value = 0.15, and falls within bootstrap distribution: Wilcoxon p-value = 0.8, Figures 2B, 2E, 2H, Table 2).

We further compared the age-adjusted proportions of positive cases in the NF1 cohort with the other selected rare diseases to test whether the lower proportions of positive cases was unique to NF1. The proportion of positive cases in the NF1 cohort was not significantly different from all the other rare disease cohorts combined (NF2, SWN, TSC, MCC, AML, FXS) (z-test p-value = 0.08, BH adjusted p-value = 0.12, falls within bootstrap distribution: Wilcoxon p-value = 1, Figure 2C, Table 2). A similar trend was noted for the SWN cohort (z-test p-value = 0.19, BH adjusted p-value = 0.19, falls within bootstrap distribution: Wilcoxon p-value = 1, Figure 2I, Table 2). Interestingly, the age-adjusted proportions of positive cases in the NF2 cohort were significantly lower compared to other rare disease cohorts (z-test p-value = 0.015, BH adjusted p-value = 0.02, falls within bootstrap distribution: Wilcoxon p-value = 0.4, Figure 2F, Table 2). Interpreting the above results conservatively, the proportions of positive cases in the N3C NF1, NF2, and SWN populations were no greater than expected for rare or non-rare diseases examined in this study.

Age-adjusted proportion of severe outcomes in NF1 was not greater than that of other diseases.

Though the positive cases did not appear to be more frequent in people with NF1, NF2, and SWN versus others, it is possible that the severity of COVID-19 in positive cases with NF1, NF2, or SWN is different from the others. In the N3C cohort, there were no patients with NF2, SWN, FXS, or TSC that had reported severe outcomes; thus, we were unable to evaluate the prevalence of severe outcomes in NF2 or SWN cohorts. We evaluated the severity of COVID-19 manifestations in the NF1 cohort and compared that to other selected cohorts. N3C has made extensive efforts to capture the severity of disease incorporating information from EHRs such as hospitalization, invasive ventilation, extracorporeal membrane oxygenation, hospice, and death.[8] We examined patient severity scores built on these parameters in our selected cohorts to estimate the severity of COVID-19.

We first identified the patients in the previously examined disease cohorts with highest documented severity[28] (N3C severity type Severe, i.e., WHO severity 7-9, and Mortality/Hospice, i.e., WHO severity 10). We then compared the age-adjusted proportions of patients with these severity types (henceforth referred to as “severe outcomes”) among positive cases in each cohort (Supplementary figure 2A-C, Supplemental Table 12). We found that the proportion of severe outcomes in the NF1 cohort was not significantly different when compared to all other cohorts (Wilcoxon test, observed p-value = 0.56, BH adjusted p-value = 0.56, falls within bootstrap distribution: p-value = 0.8) (Supplementary figure 2A, Table 3). In contrast, we found that the DM1

cohort had higher proportions of patients with severe outcomes compared to the other selected cohorts (Wilcoxon rank sum test, observed p-value = 0.003, BH adjusted p-value = 0.009, falls within bootstrap distribution: p-value = 1.0) (Supplementary figure 2B, Table 3). This finding is consistent with the now established association between diabetes and severity of COVID-19 outcomes[29,30]. The proportion of patients with severe outcomes in the NF1 cohort was not significantly higher than the other rare disease cohorts examined, suggesting no clear relationship between NF1 and severe outcome from COVID-19 infection/disease (Wilcoxon test, observed p-value = 0.04, BH adjusted p-value = 0.06, falls within bootstrap distribution: p-value = 0.28) (Supplementary figure 2C, Table 3).

We also examined the proportions of positive cases in the NF1 cohort who received invasive ventilation (Supplementary figure 2D-F, Table 3, Supplemental Table 13). The proportions requiring invasive ventilation among the positive cases in the NF1 cohort were not significantly different from the other cohorts (Wilcoxon test, observed p-value = 0.91, BH adjusted p-value = 0.92, falls within bootstrap distribution: p-value = 1.0, Supplementary figure 2D, F, & Table 3). In contrast, the DM1 cohort appears to have more invasive ventilation (Wilcoxon test, observed p-value = 0.0002, BH adjusted p-value = 0.0006) (Supplementary figure 2E, Table 3). The median length of hospital stays for the patients with NF1 who had severe outcomes was not substantially different from other cohorts (NF1: 10 days, AML: 9 days, MCC: 23 days, Non-NF1: 11 days, DM1: 13 days, HYP: 11 days, TSC: not determined., FXS: not determined., NF2: not determined., SWN: not determined.; Wilcoxon test p-value = 0.55, Supplemental Table

14). Thus, our findings suggest that the proportion of positive cases in the NF1 cohort experiencing severe outcomes was not significantly greater than the non-rare or rare disease cohorts.

DISCUSSION:

This study examined EHR data in the N3C Data Enclave to determine the burden of SARS-CoV-2 in people with NF1, NF2, and SWN. Our findings suggest that the proportion of cases of SARS-CoV-2 infection or COVID-19, and severe outcomes among patients with NF1, NF2, and SWN in the N3C Data Enclave was not higher than other selected rare and non-rare diseases when adjusted for age and site.

The N3C is the largest centralized and harmonized EHR repository of a representative COVID-19 cohort in the United States[8], well suited for studying COVID-19 related outcomes. While an extensive collection of EHR data, N3C dataset has various limitations in determining SARS-CoV-2 and COVID-19-related risks for the global population. For example, N3C shows a greater NF1 prevalence compared to population prevalence estimates, indicating that this dataset may not represent the general population due to its specific data acquisition protocols. As with any multi-site combination of EHR data, there may also be site-related differences in clinical measures due to variations in clinical practice and medical record documentation. Any biases affecting analyses of care patterns or outcomes due to geographical, regional, cultural, or other differences between institutions remained unassessed due to anonymized coding data from contributing institutions in this de-identified dataset.

Furthermore, clinical coding of patients with NF1, NF2, SWN or other rare diseases may be incomplete in EHRs, i.e., the N3C may miss disease-positive patients without appropriately recorded diagnostic codes. Conversely, rare disease patients who are control cases may be more likely to visit the healthcare system compared to people who are control cases but belong to other disease cohorts, thus impacting the proportion estimates in this study. Lastly, the SARS-CoV-2 testing rate, COVID-19 diagnosis and treatment, access to clinical care in different sites and disease populations may vary.

In addition, there are various data-specific considerations which could also introduce bias. Due to N3C's phenotype acquisition design, the patients included in N3C were matched by demographics but not disease type. This matching strategy suggests that the N3C may not provide an accurate proportion of the SARS-CoV-2 negative/non-COVID-19 population for different disease cohorts, limiting the comparisons to those across different disease cohorts within the N3C. Additionally, since the matching of two controls to each positive case was done at the time of data deposition, at each participating site, and occurred in three rounds using progressively looser requirements for the match (see Case-control matching in Methods), there may be subtle differences in the cohorts despite the best efforts of the phenotype acquisition team in N3C. It is also important to note that the definition of "SARS-CoV-2-positive or COVID-19 patients" in this study is subject to limitations such as potential false positives, false negatives, and untested asymptomatic individuals. In the presence of at-home testing, it is also likely that people identified as controls may have had COVID-19, but tested outside of their health system, or at home. Due to this caveat, which is not addressable

within the construct of the N3C study, it is necessary to assume that the controls are patients who have not had documented instances of COVID-19. This dataset also lacks records of individuals who did not have a clinical encounter at N3C contributing sites due to being suspected positive or asymptomatic. Furthermore, this study only focuses on the acute data related to SARS-CoV-2 infections and associated critical care usage. Future analyses evaluating additional patient covariates known to impact SARS-CoV-2 outcomes, such as pregnancy[31], social determinants of health (including socio-economic status, insurance status, and access to healthcare), or long-COVID data may help us refine the results of this study. Finally, sample sizes for certain diseases (e.g. FXS), makes interpretation of the results for these diseases challenging. Additional data for the cohorts may also allow higher CI estimates for comparisons in the study where the present data only enabled 60% CI calculations.

Despite these limitations, we recapitulated well-established associations between COVID-19 and DM1 (one of our control cohorts), suggesting that our methods can identify underlying patterns of SARS-CoV-2 risk and severity in a common disease.[29,30,32,33] Similar to previous observations, our findings suggest that while the proportion of DM1 patients found to be positive cases is not greater than the general population (Figure 2C), the proportion of positive cases in the DM1 cohort experiencing severe outcomes was higher compared to the rest of the comparison cohorts (Supplementary figure 2B, E, Table 2,3). These observations in our analysis are reassuring and indicate that our analytical methods may be tolerant of the inherent

biases and limitations of the N3C dataset and EHR data while identifying robust patterns for selected cohorts.

Very few studies have investigated the effect of COVID-19 on rare diseases due to the challenges in collecting information regarding rare disease cohorts. Recently, a prospective multi-center questionnaire study (4 centers) was published with 48 patients from lysosomal storage disorders presenting a descriptive assessment of the impact of the pandemic restrictions on the disease population, and their treatment adherence[34]. Similar to our study and other rare disease studies, the authors of this study also struggled with the limited size of the cohort. Additionally, they highlighted that 1) the study assessed patients at a time when the healthcare system had not yet faced massive influx of COVID-19 patients, 2) there was absence of a control cohort, such as healthy individuals or patients harboring other chronic conditions. The authors suggested that evaluating larger cohorts of patients and comparing them to relevant control cohorts was essential. As a result, this study focused mainly on descriptive analysis of the data from their cohort.

Our study is also a multicenter study (59 clinical sites) that used observational retrospective data from different rare disease cohorts to quantitatively assess the occurrence of COVID-19. We were fortunate to overcome many of the above limitations due to the centralized efforts of N3C and present a quantitative assessment of the occurrence of COVID-19 in rare disease patients. First, while our cohorts were still very small (requiring complex statistical analyses) they were still significantly larger than the

cohorts examined earlier for rare diseases. Second, the current study assesses patient data obtained between 2018 and 2021 thus capturing the peak of the COVID-19 related patient influx and the early stages of the pandemic. Our study also struggled with evaluating populations who never had COVID-19 or SARS-CoV-2 (given the lack of data from at-home testing or testing outside the clinical sites included in the study), but was able to contrast the cohorts of NF1, NF2, and SWN patients with cohorts of other rare diseases like FXS, AML, MCC, as well as non-rare diseases like DM1 and HYP.

In the future, additional studies (e.g., case-control health surveys, mobile health studies) may allow more accurate determination of the prevalence of COVID-19 and its impact on health in people with NF1, NF2, and SWN. Future studies should also evaluate whether people with rare diseases exhibit cautious behavior or stronger adherence to social distancing protocols contributing to lower SARS-CoV-2 infection rates.
This study leverages a new and unique dataset and overcomes various statistical challenges to assess COVID-19 burden and severity in a rare disease population. We anticipate that the strategies used in this study can be easily extended to examine other rare diseases of interest using the N3C dataset, thus serving as a roadmap for future work. As noted in the results, the number of NF1 patients permitted more granular analyses than with NF2 and SWN suggesting that cohort sizes over 1500 individuals from the N3C database are perhaps more feasible to study than those under 1000. As more data is added to the N3C dataset and more concept sets of rare diseases are generated and validated by clinical experts, we anticipate the role of COVID-19 in rare diseases will become easier to evaluate using N3C. Using these methods, we discovered that people with NF1, NF2, and SWN do not appear to be at a greater risk of

becoming positive cases or developing severe complications of COVID-19 compared to other rare or non-rare diseases. These findings suggest that while no elevated risk was noted as per the composition of N3C patient population in July 2021, it is important for people with NF to follow COVID-19-related public health measures, vaccination guidelines, and recommendations from NF specialists.[35]

CODE AND DATA AVAILABILITY:

Data are available in the N3C Data Enclave (https://covid.cd2h.org/enclave). All the R code used in the analyses in this study is available on GitHub (https://github.com/jaybee84/NF-COVID-response).

ACKNOWLEDGEMENTS:

Authorship was determined using ICMJE recommendations. We thank the Children's Tumor Foundation Clinical Care Advisory Board for their support and input during conceptualization of this project. We thank Dr. Tim Bergquist, Yao Yan, and Dr. Justin Guinney at Sage Bionetworks for helpful input during the design of this project. We additionally thank Dr. Harold Lehmann (Johns Hopkins School of Medicine), and Dr. Kenneth Wilkins (NIDDK) for helpful and insightful discussions regarding the statistical analysis strategies described in this study.

N3C Attribution

The analyses described in this publication were conducted with data or tools accessed through the NCATS N3C Data Enclave https://covid.cd2h.org and N3C Attribution & Publication Policy v 1.2-2020-08-25b supported by NCATS U24 TR002306. This research was possible because of the patients whose information is included within the data and the organizations (https://ncats.nih.gov/n3c/resources/data-contribution/data-transfer-agreement-signatories) and scientists who have contributed to the on-going development of this community resource [https://doi.org/10.1093/jamia/ocaa196]."

IRB

The N3C data transfer to NCATS is performed under a Johns Hopkins University Reliance Protocol # IRB00249128 or individual site agreements with NIH. The N3C Data Enclave is managed under the authority of the NIH; information can be found at https://ncats.nih.gov/n3c/resources.

Individual Acknowledgements for Core Contributors

We gratefully acknowledge contributions from the following N3C core teams:

(Asterisks indicate leads) • Principal Investigators: Melissa A. Haendel*, Christopher G. Chute*, Kenneth R. Gersing, Anita Walden

• Workstream, subgroup and administrative leaders: Melissa A. Haendel*, Tellen D. Bennett, Christopher G. Chute, David A. Eichmann, Justin Guinney, Warren A. Kibbe, Hongfang Liu, Philip R.O. Payne, Emily R. Pfaff, Peter N. Robinson, Joel H. Saltz, Heidi Spratt, Justin Starren, Christine Suver, Adam B. Wilcox, Andrew E. Williams, Chunlei Wu

• Key liaisons at data partner sites

• Regulatory staff at data partner sites

• Individuals at the sites who are responsible for creating the datasets and submitting data to N3C

• Data Ingest and Harmonization Team: Christopher G. Chute*, Emily R. Pfaff*, Davera Gabriel, Stephanie S. Hong, Kristin Kostka, Harold P. Lehmann, Richard A. Moffitt, Michele Morris, Matvey B. Palchuk, Xiaohan Tanner Zhang, Richard L. Zhu

• Phenotype Team (Individuals who create the scripts that the sites use to submit their data, based on the COVID and Long COVID definitions): Emily R. Pfaff*, Benjamin Amor, Mark M. Bissell, Marshall Clark, Andrew T. Girvin, Stephanie S. Hong, Kristin

Kostka, Adam M. Lee, Robert T. Miller, Michele Morris, Matvey B. Palchuk, Kellie M. Walters

• Project Management and Operations Team: Anita Walden*, Yooree Chae, Connor Cook, Alexandra Dest, Racquel R. Dietz, Thomas Dillon, Patricia A. Francis, Rafael Fuentes, Alexis Graves, Julie A. McMurry, Andrew J. Neumann, Shawn T. O'Neil, Usman Sheikh, Andréa M. Volz, Elizabeth Zampino

• Partners from NIH and other federal agencies: Christopher P. Austin*, Kenneth R. Gersing*, Samuel Bozzette, Mariam Deacy, Nicole Garbarini, Michael G. Kurilla, Sam G. Michael, Joni L. Rutter, Meredith Temple-O'Connor

• Analytics Team (Individuals who build the Enclave infrastructure, help create codesets, variables, and help Domain Teams and project teams with their datasets): Benjamin Amor*, Mark M. Bissell, Katie Rebecca Bradwell, Andrew T. Girvin, Amin Manna, Nabeel Qureshi

• Publication Committee Management Team: Mary Morrison Saltz*, Christine Suver*, Christopher G. Chute, Melissa A. Haendel, Julie A. McMurry, Andréa M. Volz, Anita Walden

• Publication Committee Review Team: Carolyn Bramante, Jeremy Richard Harper, Wenndy Hernandez, Farrukh M Koraishy, Federico Mariona, Amit Saha, Satyanarayana Vedula

Data Partners with Released Data

Stony Brook University — U24TR002306 • University of Oklahoma Health Sciences Center — U54GM104938: Oklahoma Clinical and Translational Science Institute (OCTSI) • West Virginia University — U54GM104942: West Virginia Clinical and Translational Science Institute (WVCTSI) • University of Mississippi Medical Center — U54GM115428: Mississippi Center for Clinical and Translational Research (CCTR) • University of Nebraska Medical Center — U54GM115458: Great Plains IDeA-Clinical & Translational Research • Maine Medical Center — U54GM115516: Northern New England Clinical & Translational Research (NNE-CTR) Network • Wake Forest University Health Sciences — UL1TR001420: Wake Forest Clinical and Translational Science Institute • Northwestern University at Chicago — UL1TR001422: Northwestern University Clinical and Translational Science Institute (NUCATS) • University of Cincinnati — UL1TR001425: Center for Clinical and Translational Science and Training • The University of Texas Medical Branch at Galveston — UL1TR001439: The Institute for Translational Sciences • Medical University of South Carolina — UL1TR001450: South Carolina Clinical & Translational Research Institute (SCTR) • University of Massachusetts Medical School Worcester — UL1TR001453: The UMass Center for Clinical and Translational Science (UMCCTS) • University of Southern California — UL1TR001855: The Southern California Clinical and Translational Science Institute (SC CTSI) • Columbia University Irving Medical Center — UL1TR001873: Irving Institute for Clinical and Translational Research • George Washington Children's Research Institute — UL1TR001876: Clinical and Translational Science Institute at Children's National (CTSA-CN) • University of Kentucky — UL1TR001998: UK Center for Clinical and

Translational Science • University of Rochester — UL1TR002001: UR Clinical & Translational Science Institute • University of Illinois at Chicago — UL1TR002003: UIC Center for Clinical and Translational Science • Penn State Health Milton S. Hershey Medical Center — UL1TR002014: Penn State Clinical and Translational Science Institute • The University of Michigan at Ann Arbor — UL1TR002240: Michigan Institute for Clinical and Health Research • Vanderbilt University Medical Center — UL1TR002243: Vanderbilt Institute for Clinical and Translational Research • University of Washington — UL1TR002319: Institute of Translational Health Sciences • Washington University in St. Louis — UL1TR002345: Institute of Clinical and Translational Sciences • Oregon Health & Science University — UL1TR002369: Oregon Clinical and Translational Research Institute • University of Wisconsin-Madison — UL1TR002373: UW Institute for Clinical and Translational Research • Rush University Medical Center — UL1TR002389: The Institute for Translational Medicine (ITM) • The University of Chicago — UL1TR002389: The Institute for Translational Medicine (ITM) • University of North Carolina at Chapel Hill — UL1TR002489: North Carolina Translational and Clinical Science Institute • University of Minnesota — UL1TR002494: Clinical and Translational Science Institute • Children's Hospital Colorado — UL1TR002535: Colorado Clinical and Translational Sciences Institute • The University of Iowa — UL1TR002537: Institute for Clinical and Translational Science • The University of Utah — UL1TR002538: Uhealth Center for Clinical and Translational Science • Tufts Medical Center — UL1TR002544: Tufts Clinical and Translational Science Institute • Duke University — UL1TR002553: Duke Clinical and Translational Science Institute • Virginia Commonwealth University — UL1TR002649: C. Kenneth

and Dianne Wright Center for Clinical and Translational Research • The Ohio State University — UL1TR002733: Center for Clinical and Translational Science • The University of Miami Leonard M. Miller School of Medicine — UL1TR002736: University of Miami Clinical and Translational Science Institute • University of Virginia — UL1TR003015: iTHRIV Integrated Translational health Research Institute of Virginia • Carilion Clinic — UL1TR003015: iTHRIV Integrated Translational health Research Institute of Virginia • University of Alabama at Birmingham — UL1TR003096: Center for Clinical and Translational Science • Johns Hopkins University — UL1TR003098: Johns Hopkins Institute for Clinical and Translational Research • University of Arkansas for Medical Sciences — UL1TR003107: UAMS Translational Research Institute • Nemours — U54GM104941: Delaware CTR ACCEL Program • University Medical Center New Orleans — U54GM104940: Louisiana Clinical and Translational Science (LA CaTS) Center • University of Colorado Denver, Anschutz Medical Campus — UL1TR002535: Colorado Clinical and Translational Sciences Institute • Mayo Clinic Rochester — UL1TR002377: Mayo Clinic Center for Clinical and Translational Science (CCaTS) • Tulane University — UL1TR003096: Center for Clinical and Translational Science • Loyola University Medical Center — UL1TR002389: The Institute for Translational Medicine (ITM) • Advocate Health Care Network — UL1TR002389: The Institute for Translational Medicine (ITM) • OCHIN — INV-018455: Bill and Melinda Gates Foundation grant to Sage Bionetworks

Additional Data Partners Who Have Signed a DTA and Whose Data Release is Pending

The Rockefeller University — UL1TR001866: Center for Clinical and Translational Science • The Scripps Research Institute — UL1TR002550: Scripps Research

Translational Institute • University of Texas Health Science Center at San Antonio — UL1TR002645: Institute for Integration of Medicine and Science • The University of Texas Health Science Center at Houston — UL1TR003167: Center for Clinical and Translational Sciences (CCTS) • NorthShore University HealthSystem — UL1TR002389: The Institute for Translational Medicine (ITM) • Yale New Haven Hospital — UL1TR001863: Yale Center for Clinical Investigation • Emory University — UL1TR002378: Georgia Clinical and Translational Science Alliance • Weill Medical College of Cornell University — UL1TR002384: Weill Cornell Medicine Clinical and Translational Science Center • Montefiore Medical Center — UL1TR002556: Institute for Clinical and Translational Research at Einstein and Montefiore • Medical College of Wisconsin — UL1TR001436: Clinical and Translational Science Institute of Southeast Wisconsin • University of New Mexico Health Sciences Center — UL1TR001449: University of New Mexico Clinical and Translational Science Center • George Washington University — UL1TR001876: Clinical and Translational Science Institute at Children's National (CTSA-CN) • Stanford University — UL1TR003142: Spectrum: The Stanford Center for Clinical and Translational Research and Education • Regenstrief Institute — UL1TR002529: Indiana Clinical and Translational Science Institute • Cincinnati Children's Hospital Medical Center — UL1TR001425: Center for Clinical and Translational Science and Training • Boston University Medical Campus — UL1TR001430: Boston University Clinical and Translational Science Institute • The State University of New York at Buffalo — UL1TR001412: Clinical and Translational Science Institute • Aurora Health Care — UL1TR002373: Wisconsin Network For Health Research • Brown University — U54GM115677: Advance Clinical Translational

Research (Advance-CTR) • Rutgers, The State University of New Jersey — UL1TR003017: New Jersey Alliance for Clinical and Translational Science • Loyola University Chicago — UL1TR002389: The Institute for Translational Medicine (ITM) • #N/A — UL1TR001445: Langone Health's Clinical and Translational Science Institute • Children's Hospital of Philadelphia — UL1TR001878: Institute for Translational Medicine and Therapeutics • University of Kansas Medical Center — UL1TR002366: Frontiers: University of Kansas Clinical and Translational Science Institute • Massachusetts General Brigham — UL1TR002541: Harvard Catalyst • Icahn School of Medicine at Mount Sinai — UL1TR001433: ConduITS Institute for Translational Sciences • Ochsner Medical Center — U54GM104940: Louisiana Clinical and Translational Science (LA CaTS) Center • HonorHealth — None (Voluntary) • University of California, Irvine — UL1TR001414: The UC Irvine Institute for Clinical and Translational Science (ICTS) • University of California, San Diego — UL1TR001442: Altman Clinical and Translational Research Institute • University of California, Davis — UL1TR001860: UCDavis Health Clinical and Translational Science Center • University of California, San Francisco — UL1TR001872: UCSF Clinical and Translational Science Institute • University of California, Los Angeles — UL1TR001881: UCLA Clinical Translational Science Institute • University of Vermont — U54GM115516: Northern New England Clinical & Translational Research (NNE-CTR) Network • Arkansas Children's Hospital — UL1TR003107: UAMS Translational Research Institute

AUTHOR INFORMATION:

Authorship was determined using ICMJE recommendations.

Conceptualization - J.B., L.K., K.Y., J.T.J, S.P., J.M.F., R.J.A., J.O.B.;

Data curation - J.B.;

Formal Analysis - J.B.;

Funding acquisition - J.B., R.J.A, J.O.B;

Investigation - J.B., R.J.A;

Methodology - J.B., J.M.F, R.J.A.;

Project administration - J.B., R.J.A., J.O.B.;

Resources - J.B., R.J.A;

Software - J.B.;

Supervision - R.J.A., J.O.B.;

Validation - J.B.;

Visualization - J.B.;

Writing – original draft - J.B., J.M.F., R.J.A., J.O.B.;

Writing – review & editing- J.B., L.K., K.Y., J.T.J., S.P., J.M.F., R.J.A., J.O.B.

ETHICS DECLARATION:

Data access and analysis in this study were compliant with the research protocol (Sage Bionetworks #2021101002) approved by the Western Institutional Review Board - Copernicus Group IRB (WCG IRB) and granted IRB-exempt status. Subsequently a request (#RP-DD0EDC, 'Investigating COVID-19 burden in neurofibromatosis type 1 patients') for access to the de-identified N3C dataset (phenotypic acquisition v3.3) was submitted and approved by the N3C Enclave Data Access Committee.

Clinical institutions with formally executed data transfer agreements with the National Center for Advancing Translational Sciences (NCATS) (https://ncats.nih.gov/n3c/resources/data-contribution/data-transfer-agreement-signatories) contributed de-identified and retrospective electronic health record data associated with a limited set of patients relevant to COVID-19. As the steward of the data, NCATS oversees the use of the data and the FedRAMP certified N3C Data Enclave through user registration, federated login, data use agreements with institutions and data use requests with users. Thus, the data utilized in the study did not require informed consent from individual patients. This study does not include any individual patient information, all analyses use aggregated and de-identified information.

DISCLOSURES:

Justin T Jordan is a recipient of royalties from Elsevier, and consulting fees from Navio Theragnostics, CereXis, and Recursion Inc.

Scott Plotkin is co-founder of NFlection Therapeutics, NF2 Therapeutics; consults for Akouos; and serves on the Scientific Advisory Board and holds stock in SonALAsense.

FIGURES:

Figure 1

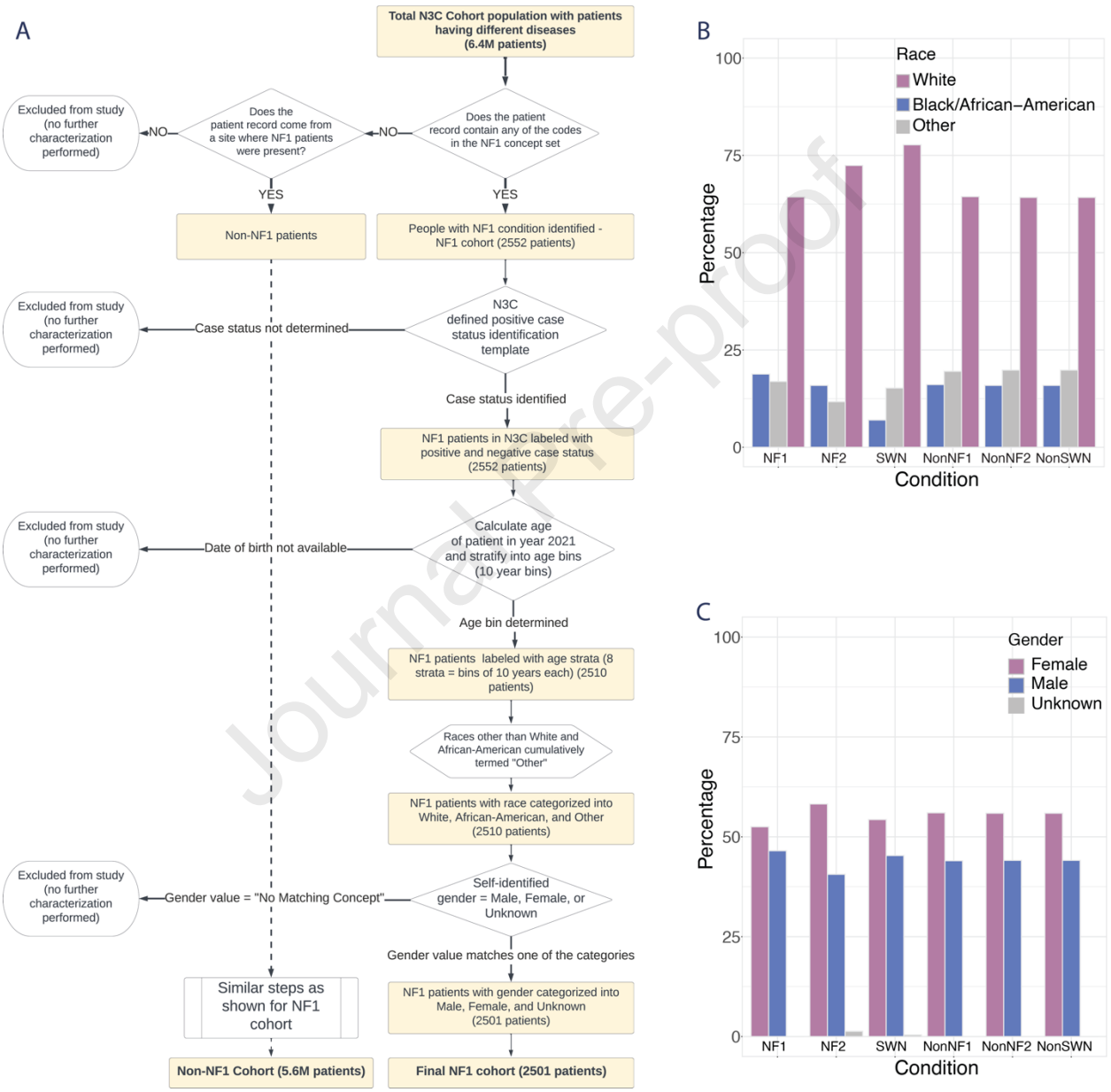

Figure 1. Demographics of selected cohorts in N3C. (A) An example flow diagram showing the various stages of selection of patients to generate the NF1 cohort. The

number of patients at each stage is noted. Similar steps were taken during generation of other cohorts in this study. (B) Bar-plot showing percentage of unique persons that identify as White, Black, or Other races in the selected cohorts. (NF1: Neurofibromatosis type 1, Non-NF1: general population without NF1, Non-NF2: general population without NF2, Non-SWN: general population without SWN) (C) Bar-plot showing percentage of unique persons identifying as Male or Female in NF1, NF2, SWN, Non-NF1, Non-NF2, and Non-SWN cohorts.

Figure 2

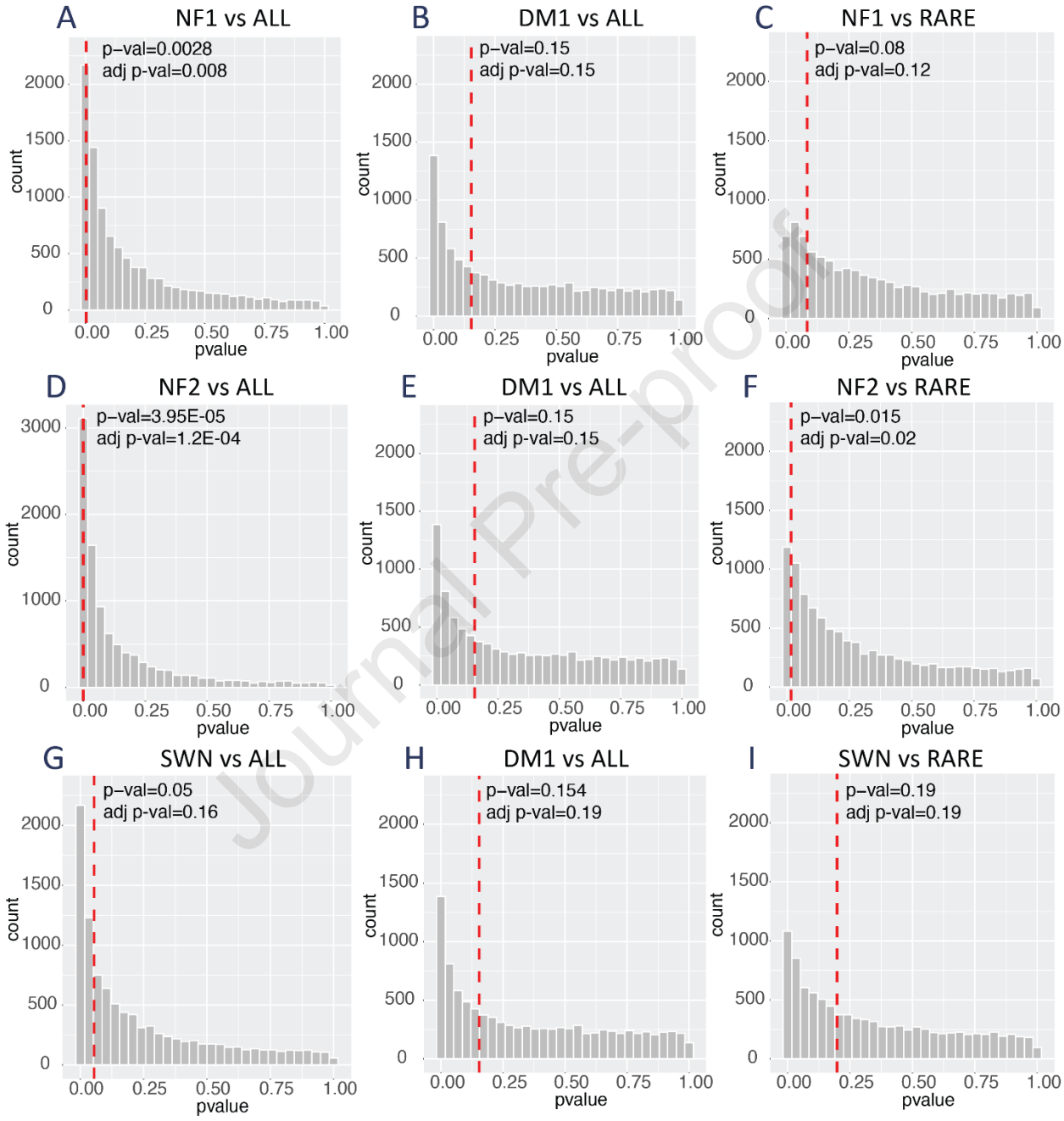

Figure 2. Comparison of age-adjusted proportions of positive cases in selected cohorts. Selected cohorts include NF1: Neurofibromatosis type 1, TSC: tuberous

sclerosis, AML: acute myeloid leukemia, FXS: fragile-X syndrome, MCC: Merkel cell carcinoma, Non-NF1/Non-NF2/Non-SWN: general population, DM1: diabetes mellitus type 1, HYP: controlled hypertension (A-C) Results of the bootstrap analysis for p-value of comparisons between NF1 and all, DM1 vs. all, NF1 vs. rare disease cohorts. (D-F) Results of the bootstrap analysis for comparisons between NF2 and all, DM1 vs all, NF2 vs rare disease cohorts. (G-I) Results of the bootstrap analysis for comparisons of p-values between SWN and all, DM1 vs. all, SWN vs rare disease cohorts. The red dashed line represents the p-value obtained from the real observations. The specific and adjusted value for each comparison is noted in the plot inset. The grey bars show a histogram of all possible p-values obtained through 10,000 iterations of bootstrap analysis.

Table 1.

	NF1	NF2	SWN	TSC	AML	FXS	MCC	Non-NF1	Non-NF2	Non-SWN	DM1	HYP
Site-adjusted Cohort Size	2,501	665	762	861	9,844	98	648	5,577,737	5,579,215	5,579,146	66,234	1,664,134
Site-adjusted total positive cases	352	97	118	149	1,595	26	103	1,621,928	1,622,133	1,622,123	17,091	435,562
Median Age (years)	28	49	60	23	62	28	75	46	46	46	50	63
Age-adjusted counts of positive cases per 100,000 US standard population	14,496	13,782	13,738	19,346	18,135	28,105	19823	28,503	28,498	28,498	24,022	24,949
Approximate percentage of positive cases	14.5	13.8	13.7	19.3	18.1	28.1	19.8	28.5	28.5	28.5	24.0	24.9

Table 1: **Table showing the number of unique persons and the age-adjusted counts and percentages of positive cases in each selected cohort.** (NF1:

Neurofibromatosis type 1, TSC: tuberous sclerosis, AML: acute myeloid leukemia, FXS: fragile-X syndrome, MCC: Merkel cell carcinoma, Non-NF1: general population without NF1, Non-NF2: general population without NF2, Non-SWN: general population without SWN, DM1: diabetes mellitus type-1, HYP: controlled hypertension)

Table 2:

Comparison	Age-adjusted counts of positive cases in target disease (per 100,000)	z-test p-value	Estimate (difference in mean between groups)	95% CI (lower) of estimate	95% CI (upper) of estimate	adjusted z-test p-value	Wilcoxon p-value (bootstrap)	Estimate (difference in location parameter between groups (bootstrap)	60% CI (lower) of estimate (bootstrap)	60% CI (upper) of estimate (bootstrap)
NF1 vs all	14496	0.002	-832.47	-1380.16	-284.80	0.008	0.5	-0.26	-0.97	-0.19
NF2 vs all	13782	0.00003	-931.63	-1375.85	-487.41	0.00012	0.5	-0.34	-0.60	-0.11
SWN vs all	13738	0.05	-937.65	-1894.27	18.95	0.16	1	0.002	-0.74	0.005
DM1 vs all	24022	0.15	490.63	-184.29	1165.70	0.15	0.8	0.09	-0.23	0.15
NF1 vs rare	14496	0.08	-540.66	-1153.10	71.76	0.12	0.8	-0.10	-0.79	0.05
NF2 vs rare	13782	0.015	-644.84	-1167.71	-121.98	0.02	0.4	-0.06	-0.54	0.01
SWN vs rare	13738	0.19	-651.17	-1641.66	339.31	0.19	1	0.02	-0.71	0.19

Table 2: Table showing age-adjusted counts and p-values of all comparisons of positive cases in selected cohorts (as shown in Figure 2 A-F). Confidence interval is abbreviated as CI in the table. In the bootstrap analysis, the z-test p-value was compared to a distribution of bootstrapped p-values using the non-parametric Wilcoxon rank sum test. In this test, the null hypothesis is that the two distributions differ by a location shift of μ and the alternative hypothesis is that they differ by a location shift other than μ. The "estimate" of this non-parametric test is equal to the difference in μ which in the present case has negative values due to the direction of the location shift. The confidence intervals reflect the range of μ and has negative values. The skew in the distribution of bootstrapped p-values did not allow confidence interval calculations at 95% (as the difference between $\boldsymbol{\alpha}$ achieved from the distribution and $\boldsymbol{\alpha}_{target}$ was greater than $\boldsymbol{\alpha}_{target}/2$, where $\boldsymbol{\alpha}_{target} = 0.05$), but enabled 60% CI estimation. A 60% confidence interval is more likely to reject the null hypothesis as compared to a 95% CI.

Table 3:

Comparison	Age-adjusted counts of severe outcomes in target disease (per 100,000)	Wilcoxon p-value	Estimate (difference in location parameter between groups)	95% CI (lower) of estimate	95% CI (upper) of estimate	adjusted Wilcoxon p-value	Wilcoxon p-value (bootstrap)	Estimate (difference in location parameter between groups) (bootstrap)	CI (lower) of estimate (bootstrap)	CI (upper) of estimate (bootstrap)
Severe Outcomes										
NF1 vs all	887	0.56	0.0000016	-0.00006	204.70	0.56	0.8	-0.18	-0.43 [a]	-0.04[a]
DM1 vs all	534	0.003	42.10	28.05	64.43	0.009	1	-0.07	-0.36 [a]	0.002 [a]
NF1 vs rare	887	0.04	0.000002	-0.000019	204.70	0.06	0.28	-0.04	-0.34	-0.034
Invasive Ventilation										
NF1 vs all	521	0.917	-0.0000054	-0.00008	0.00001	0.92	1	0.10	-0.08 [a]	0.28 [a]
DM1 vs all	303	0.0002	32.25	28.05	47.28	0.0006	0.4	-0.03	-0.18 [a]	-0.002 [a]
NF1 vs rare	521	0.06	0.0000038	-0.000040	0.00	0.07	0.28	-0.28	-0.93	-0.1

Table 3: Table showing age-adjusted counts, confidence intervals (CI), and p-values of all comparisons of severe outcomes and invasive ventilation recorded in selected cohorts. In some cases, the skew in the distribution of bootstrapped p-values did not allow confidence interval calculations at 95% CI (as the difference between α achieved from the distribution and α_{target} was greater than $\alpha_{target}/2$, where $\alpha_{target} = 0.05$). Confidence interval calculations at the 60% level are reported for these comparisons (indicated by [a]). The confidence limits without an asterisk denote 95% CI. A 60% confidence interval is more likely to reject the null hypothesis as compared to a 95% CI.

REFERENCES:

1. Dg, E. *et al.* Birth incidence and prevalence of tumor-prone syndromes: estimates from a UK family genetic register service. *Am. J. Med. Genet. A* **152A**, 327–332 (2010).
2. Dg, E. *et al.* Schwannomatosis: a genetic and epidemiological study. *J. Neurol. Neurosurg. Psychiatry* **89**, (2018).
3. E, U. *et al.* Distinctive Cancer Associations in Patients With Neurofibromatosis Type 1. *J. Clin. Oncol.* **34**, 1978–1986 (2016).
4. Rasmussen, S. A., Yang, Q. & Friedman, J. M. Mortality in neurofibromatosis 1: an analysis using U.S. death certificates. *Am. J. Hum. Genet.* **68**, 1110–1118 (2001).
5. Radtke, H. B. *et al.* The impact of the COVID-19 pandemic on neurofibromatosis clinical care and research. *Orphanet J. Rare Dis.* **16**, 61 (2021).
6. Wolters, P. L. *et al.* Impact of the coronavirus pandemic on mental health and health care in adults with neurofibromatosis: Patient perspectives from an online survey. *Am. J. Med. Genet. A* **188**, 71–82 (2022).
7. Haendel, M. A. *et al.* The National COVID Cohort Collaborative (N3C): Rationale, design, infrastructure, and deployment. *J. Am. Med. Inform. Assoc.* **28**, 427–443 (2021).
8. Bennett, T. D. *et al.* Clinical Characterization and Prediction of Clinical Severity of SARS-CoV-2 Infection Among US Adults Using Data From the US National COVID Cohort Collaborative. *JAMA Network Open* **4**, e2116901–e2116901 (2021).
9. Phenotype_Data_Acquisition Wiki. *Github Accessed August 11, 2021*

https://github.com/National-COVID-Cohort-Collaborative/Phenotype_Data_Acquisition.

10. Tolliver, S., Smith, Z. I. & Silverberg, N. The genetics and diagnosis of pediatric neurocutaneous disorders: Neurofibromatosis and tuberous sclerosis complex. *Clin. Dermatol.* (2022) doi:10.1016/j.clindermatol.2022.02.010.
11. Stone, W. L., Basit, H. & Los, E. Fragile X Syndrome. in *StatPearls* (StatPearls Publishing, 2022).
12. Becker, J. C. *et al.* Merkel cell carcinoma. *Nat Rev Dis Primers* **3**, 17077 (2017).
13. Pelcovits, A. & Niroula, R. Acute Myeloid Leukemia: A Review. *R. I. Med. J.* **103**, 38–40 (2020).
14. Incidence and Death Rates. https://www.cdc.gov/cancer/uscs/technical_notes/stat_methods/rates.htm.
15. Anderson, R. N. & Rosenberg, H. M. Age standardization of death rates: implementation of the year 2000 standard. *Natl. Vital Stat. Rep.* **47**, 1–16, 20 (1998).
16. SEER*Stat. https://seer.cancer.gov/seerstat/tutorials/aarates/definition.html.
17. Zhu, J. *et al.* Clinicopathological characteristics and survival outcomes in neuroendocrine prostate cancer: A population-based study. *Medicine* **100**, e25237 (2021).
18. Peckham-Gregory, E. C. *et al.* Racial/ethnic disparities and incidence of malignant peripheral nerve sheath tumors: results from the Surveillance, Epidemiology, and End Results Program, 2000-2014. *J. Neurooncol.* **139**, 69–75 (2018).
19. Marcadis, A. R., Davies, L., Marti, J. L. & Morris, L. G. T. Racial Disparities in

Cancer Presentation and Outcomes: The Contribution of Overdiagnosis. *JNCI Cancer Spectr* **4**, kaa001 (2020).

20. Peckham-Gregory, E. C. *et al.* Evaluation of racial disparities in pediatric optic pathway glioma incidence: Results from the Surveillance, Epidemiology, and End Results Program, 2000-2014. *Cancer Epidemiol.* **54**, 90–94 (2018).
21. Coombes, B. J. & Biernacka, J. M. Application of the parametric bootstrap for gene-set analysis of gene-environment interactions. *Eur. J. Hum. Genet.* **26**, 1679–1686 (2018).
22. Považan, M. *et al.* Comparison of Multivendor Single-Voxel MR Spectroscopy Data Acquired in Healthy Brain at 26 Sites. *Radiology* **295**, 171–180 (2020).
23. Halekoh, U. & Højsgaard, S. A Kenward-Roger Approximation and Parametric Bootstrap Methods for Tests in Linear Mixed Models – The R Package pbkrtest. *J. Stat. Softw.* **59**, 1–32 (2014).
24. Pirracchio, R., Resche-Rigon, M., Chevret, S. & Journois, D. Do simple screening statistical tools help to detect reporting bias? *Ann. Intensive Care* **3**, 29 (2013).
25. Pasmant, E., Vidaud, M., Vidaud, D. & Wolkenstein, P. Neurofibromatosis type 1: from genotype to phenotype. *J. Med. Genet.* **49**, 483–489 (2012).
26. Poyhonen, M., Kytölä, S. & Leisti, J. Epidemiology of neurofibromatosis type 1 (NF1) in northern Finland. *J. Med. Genet.* **37**, 632–636 (2000).
27. Kallionpää, R. A. *et al.* Prevalence of neurofibromatosis type 1 in the Finnish population. *Genet. Med.* **20**, 1082–1086 (2018).
28. WHO Working Group on the Clinical Characterisation and Management of COVID-19 infection. A minimal common outcome measure set for COVID-19 clinical

research. *Lancet Infect. Dis.* **20**, e192–e197 (2020).

29. Gregory, J. M. *et al.* COVID-19 Severity Is Tripled in the Diabetes Community: A Prospective Analysis of the Pandemic's Impact in Type 1 and Type 2 Diabetes. *Diabetes Care* **44**, 526–532 (2021).
30. Lim, S., Bae, J. H., Kwon, H.-S. & Nauck, M. A. COVID-19 and diabetes mellitus: from pathophysiology to clinical management. *Nat. Rev. Endocrinol.* **17**, 11–30 (2021).
31. Brandt, J. S. *et al.* Epidemiology of coronavirus disease 2019 in pregnancy: risk factors and associations with adverse maternal and neonatal outcomes. *Am. J. Obstet. Gynecol.* **224**, 389.e1-389.e9 (2021).
32. Richardson, S. *et al.* Presenting Characteristics, Comorbidities, and Outcomes Among 5700 Patients Hospitalized With COVID-19 in the New York City Area. *JAMA* **323**, 2052–2059 (2020).
33. Barron, E. *et al.* Associations of type 1 and type 2 diabetes with COVID-19-related mortality in England: a whole-population study. *Lancet Diabetes Endocrinol* **8**, 813–822 (2020).
34. Kristal, E. *et al.* The effects of the COVID-19 pandemic on patients with lysosomal storage disorders in Israel. *Orphanet J. Rare Dis.* **16**, 379 (2021).
35. Korf, B. Considerations for Individuals with NF Regarding the Novel Coronavirus. https://www.uab.edu/medicine/nfprogram/blog/considerations-for-individuals-with-nf-regarding-the-novel-coronavirus.

Age-adjusted counts of positive cases per 100,000 US standard population	Median Age (years)	Site-adjusted total positive cases	Site-adjusted Cohort Size	
14,496	28	352	2,501	**NF1**
13,782	49	97	665	**NF2**
13,738	60	118	762	**SWN**
19,346	23	149	861	**TS**
18,135	62	1,595	9,844	**AML**
28,105	28	26	98	**FX**
19823	75	103	648	**MCC**
28,503	46	1,621,928	5,577,737	**Non-NF1**
28,498	46	1,622,133	5,579,215	**Non-NF2**
28,498	46	1,622,123	5,579,146	**Non-SWN**
24,022	50	17,091	66,234	**DM1**
24,949	63	435,562	1,664,134	**HYP**

Approximate percentage of positive cases	14.5	13.8	13.7	19.3	18.1	28.1	19.8	28.5	28.5	28.5	24	24.9

Table 1: Table showing the number of unique persons and the age-adjusted counts and percentages of positive cases in each selected cohort. (NF1: Neurofibromatosis type 1, TS: tuberous sclerosis, AML: acute myeloid leukemia, FX: fragile-X syndrome, MCC: Merkel cell carcinoma, Non-NF1: general population without NF1, Non-NF2: general population without NF2, Non-SWN: general population without SWN, DM1: diabetes mellitus type-1, HYP: controlled hypertension)

NF1 vs rare	DM1 vs all	SWN vs all	NF2 vs all	NF1 vs all	Comparison
14496	24022	13738	13782	14496	Age-adjusted counts of positive cases in target disease (per 100,000)
0.08	0.15	0.05	0.00003	0.002	z-test p-value
-540.7	490.63	-937.65	-931.63	-832.47	Estimate (difference in mean between groups)
-1153	-184.3	-1894.3	-1375.9	-1380.2	95% CI (lower) of estimate
71.76	1165.7	18.95	-487.41	-284.8	95% CI (upper) of estimate
0.12	0.15	0.16	0.00012	0.008	adjusted z-test p-value
0.8	0.8	1	0.5	0.5	Wilcoxon p-value (bootstrap)
-0.1	0.09	0.002	-0.34	-0.26	Estimate (difference in location parameter between groups (bootstrap)
-0.79	-0.23	-0.74	-0.6	-0.97	60% CI (lower) of estimate (bootstrap)
0.05	0.15	0.005	-0.11	-0.19	60% CI (upper) of estimate (bootstrap)

NF2 vs rare	13782	0.015	-644.84	-1167.7	-121.98	0.02	0.4	-0.06	-0.54	0.01
SWN vs rare	13738	0.19	-651.17	-1641.7	339.31	0.19	1	0.02	-0.71	0.19

Table 2: Table showing age-adjusted counts and p-values of all comparisons of positive cases in selected cohorts (as shown in Figure 2 A-F). Confidence interval is abbreviated as CI in the table. In the bootstrap analysis, the z-test p-value was compared to a distribution of bootstrapped p-values using the non-parametric Wilcoxon rank sum test. In this test, the null hypothesis is that the two distributions differ by a location shift of μ and the alternative hypothesis is that they differ by a location shift other than μ. The "estimate" of this non-parametric test is equal to the difference in μ which in the present case has negative values due to the direction of the location shift. The confidence intervals reflect the range of μ and has negative values. The skew in the distribution of bootstrapped p-values did not allow confidence interval calculations at 95% (as the difference between achieved from the distribution and target was greater than target/2, where target = 0.05), but enabled 60% CI estimation. A 60% confidence interval is more likely to reject the null hypothesis as compared to a 95% CI.

DM1 vs all	NF1 vs all	Invasive Ventilation	NF1 vs rare	DM1 vs all	NF1 vs all	Severe Outcomes	Comparison
303	521		887	534	887		Age-adjusted counts of severe outcomes in target disease (per 100,000)
0.0002	0.917		0.04	0.003	0.56		Wilcoxon p-value
32.25	-0.0000054		0.000002	42.1	0.0000016		Estimate (difference in location parameter between groups)
28.05	-0.00008		-1.9E-05	28.05	-0.00006		95% CI (lower) of estimate
47.28	0.00001		204.7	64.43	204.7		95% CI (upper) of estimate
0.0006	0.92		0.06	0.009	0.56		adjusted Wilcoxon p-value
0.4	1		0.28	1	0.8		Wilcoxon p-value (bootstrap)
-0.03	0.1		-0.04	-0.07	-0.18		Estimate (difference in location parameter between groups) (bootstrap)
-0.18*	-0.08*		-0.34	-0.36*	-0.43*		CI (lower) of estimate (bootstrap)
-0.002*	0.28*		-0.034	0.002*	-0.04*		CI (upper) of estimate (bootstrap)

NF1 vs rare	521	0.06	0.0000038	-0.00004	0	0.07	0.28	-0.28	-0.93	-0.1

Table 3: Table showing age-adjusted counts, confidence intervals (CI), and p-values of all comparisons of severe outcomes and invasive ventilation recorded in selected cohorts. In some cases, the skew in the distribution of bootstrapped p-values did not allow confidence interval calculations at 95% CI (as the difference between α achieved from the distribution and α target was greater than α target/2, where α target = 0.05). Confidence interval calculations at the 60% level are reported for these comparisons (indicated by *). The confidence limits without an asterisk denote 95% CI. A 60% confidence interval is more likely to reject the null hypothesis as compared to a 95% CI.